CRYSTAL GROWTH & DESIGN

Article

pubs.acs.org/crystal

Buffer Pellets for High-Yield, Top-Seeded Melt Growth of Large Grain Y−Ba−Cu−O Superconductors

Namburi Devendra Kumar,* Yunhua Shi, Wei Zhai, Anthony R. Dennis, John H. Durrell, and David A. Cardwell

Department of Engineering, University of Cambridge, Trumpington Street, Cambridge CB2 1PZ, United Kingdom

ABSTRACT: Single-grain, (RE)−Ba−Cu−O [(RE)BCO)] bulk high-temperature superconductors have significant potential for application as trapped field magnets in a range of engineering devices. However, it is not trivial to fabricate single grains of (RE)BCO due to the complexity of the growth process, especially when the sample diameter exceeds 25 mm. In particular, difficulties associated with the seed crystal can lead to poor grain growth or to complete growth failure. We have employed an optimized buffer technique, which was determined by optimizing targeted critical parameters of the buffer pellet, including the choice of the buffer pellet composition and its aspect ratio, for the reliable fabrication of large, single grains of (RE)BCO. Potential candidates for the buffer pellet composition have been identified to yield successful grain growth and good superconducting properties. The optimum aspect ratio of the buffer pellet was also determined as part of this study. The optimized buffer pellet capped with the seed crystal has been demonstrated to work effectively as an efficient seed crystal and to aid significantly the growth of the Y-123 phase. We show that this optimized buffer technique ameliorates problems associated with both interfacial stress (commonly occurring at the seed/sample interface) and problems of grain contamination. We have fabricated a 40.8 mm diameter single-grain bulk superconductor and more than 25 single-grain YBCO samples with diameters in the range 25−35 mm by a significantly improved top-seeded melt growth process.

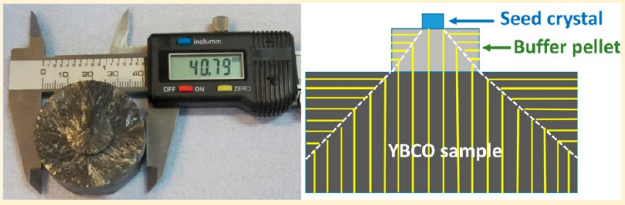

1. INTRODUCTION

The top-seeded melt growth (TSMG) process is a well-established route for the fabrication of bulk Y−Ba−Cu−O (YBCO) superconductors that can carry large critical current densities and generate large trapped magnetic fields.[1−4] It is well-known that these materials exhibit a critical current density, J_c, as large as 10^4 to 10^5 A/cm^2 within the grain, even at liquid nitrogen temperatures, 77 K.[5,6]

Unfortunately, the presence of grain boundaries has an adverse effect on the superconducting properties of polycrystalline YBCO samples by reducing the magnitude of J_c by as much as 2 to 3 orders of magnitude.[7] It is necessary, therefore, to eliminate grain boundaries from the bulk YBCO microstructure if these materials are to support large supercurrent loops that flow over large areas to generate a large magnetic moment and hence a large trapped magnetic field. Theoretically, the trapped field, B_t, varies as $B_t \propto J_c \times r$, where r is the radius of the supercurrent loop, which indicates that it is desirable to have either a large value of J_c, a large value of r, or a large value of both parameters for optimum performance. As a result, it is highly desirable to fabricate bulk YBCO superconductors in the form of large, single grains with high J_c values.

In practice, the maximum value of J_c for YBCO is determined by various microstructural features, including the nature and size of nonsuperconducting inclusions,[8] the presence of defects, such as twins,[9] twin boundaries,[10] and nanodefects,[11] and oxygen deficient regions,[12] which can provide effective flux pinning sites and resist the Lorentz force in the presence of a magnetic field. In general, however, engineering of the YBCO sample microstructure to provide increased flux pining is difficult and invariably further complicates an existing and difficult materials process.

Increasing sample size to increase trapped field, on the other hand (i.e., increasing the radius of the supercurrent loop), is a more practical option for achieving larger trapped fields. This, again, is an involved task since the growth of the superconducting $YBa_2Cu_3O_{7-x}$ (Y-123) phase is relatively complicated and depends on various growth parameters.[6,13] Y-123 melts incongruently when heated above its peritectic temperature, T_p (1005 °C in air), and decomposes into a solid Y_2BaCuO_5 (Y-211) phase and a barium-rich liquid phase comprising $BaCuO_2$ and CuO. These phases recombine to form Y-123 on subsequent cooling of the material below T_p. In general, this process often generates multiple grain nucleation sites, resulting in the formation of a multigrained YBCO microstructure. As a consequence, a seeding technique has been developed over the past 25 years to enable the fabrication of large, single-grain bulk superconductors.[14] Suitable seed crystals are required to exhibit certain features to effectively nucleate epitaxial grain growth, including a similar crystal structure to that of the Y-123 phase, phase stability, and higher melting temperature growth.[15,16] Fortunately, for the YBCO system, these criteria are satisfied by both Nd-123 and Sm-123 phase

Received: December 12, 2014
Published: January 19, 2015

DOI: 10.1021/cg501813y
Cryst. Growth Des. 2015, 15, 1472−1480

compounds, which have a higher T_p than that of Y-123 (1068 and 1054 °C, respectively). In addition, Mg-doped Nd-123 generic seed crystals have been developed recently to aid the TSMG processing of all (RE)BCO bulk superconductors (where RE is a rare earth element, such as Nd, Sm, or Gd).[17] Thin films of MgO[18−20] and NdBCO/YBCO/MgO[21,22] have also been investigated for their use as potential seed crystals in the YBCO and SmBCO systems, but Mg from the thin film seed crystal substrate can diffuse into the parent bulk and thus can cause contamination problems.

Epitaxial single grains of YBCO can now be fabricated routinely by TSMG employing a suitable seed crystal, which is placed on the top surface of the precursor pellet at room temperature (so-called cold seeding) and by subsequently cooling the sample slowly through the peritectic solidification temperature after decomposition. However, this is an involved process, and the optimization of many parameters, such as choice of seed, homogeneity of precursor powders, the use of grain refiners, etc., is critical to the growth process. A small disturbance in the growth conditions in the vicinity of the growth front, for example, can affect adversely the single-grain growth process itself and result in incomplete or multigrain growth. Figure 1 shows photographs of a selection of failed YBCO samples to illustrate the complexity of the TSMG process.

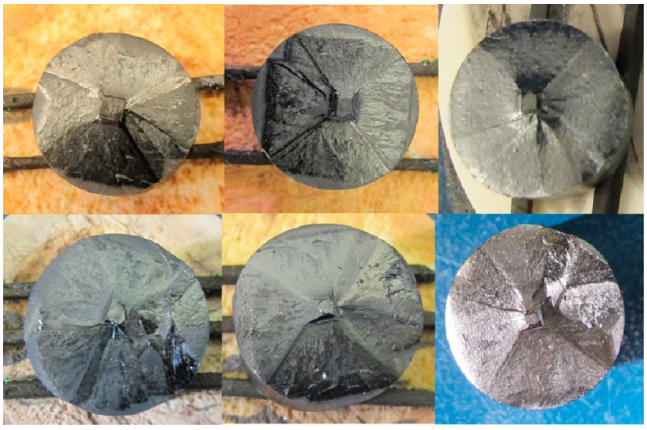

Figure 1. Photographs of a selection of failed YBCO samples to illustrate the complexity of the TSMG process.

The effects of seed dimensions on the growth of the Y-123 phase have been studied by Kim et al. in an attempt to fabricate larger single grains.[23] The results of this study show that larger and thicker seed crystals generally yield improved, more controlled growth of Y-123. However, it is difficult to fabricate seed crystals that exhibit these properties consistently, with thicker seeds containing more imperfections. On the other hand, thinner seed crystals tend to melt relatively easily under the influence of corrosive liquid phases at elevated temperature during melt processing. Indeed, seeds can melt at temperatures below their actual melting temperature[24] due to the formation of a non-equilibrium state in the presence of the Ba-rich liquid phase. Many factors, such as the seeding method, holding time at temperature, composition of the seed, the precursor pellet, etc., can further influence the melting temperature of the seed crystal. The growth process becomes more complicated still when large sized bulk samples are to be fabricated (for example, samples of diameter >25 mm) and is influenced critically by the following factors:

(i) the slow growth rate of the Y-123 phase;
(ii) non-availability of a source of yttrium, which is critical during the growth of the Y-123 phase;
(iii) the formation of subgrains in the system;
(iv) non-uniformity in the distribution of heat across the volume of a large sample;
(v) appropriate choice of seed.

It has also been observed that Nd-123/Sm-123 seeds often contaminate the main (RE)BCO system by the diffusion of Nd/Sm, which tends to form solid solutions that reduce the uniformity of $J_c(B)$ across the sample volume.[25] This potentially serious problem has been addressed partly by employing a buffer pellet between the seed crystal and the precursor pellet.[26,27] In the present article, we investigate the TSMG process using a buffer layer as follows:

(i) To determine if the buffer pellet really aids the growth of the Y-123 phase;
(ii) to determine an effective composition for the buffer pellet;
(iii) to investigate the aspect ratio of the buffer pellet on the growth process;
(iv) to determine whether the buffer pellet can negate the effects of any small defects present in the seed crystal.

The results of this study demonstrate clearly that large, single-grain bulk YBCO superconductors with a diameter up to 40.8 mm can be melt-processed easily and routinely with a very high success rate (>95%) by employing a buffer layer pellet of optimized composition.

2. EXPERIMENTAL SECTION

Commercial Y-123 (3N, Toshima), Y-211 (3N, Toshima), and CeO_2 (3N, Alfa Aesar) powders were used as initial precursors to fabricate single grain bulk superconductors. The size of the Y-123 and Y-211 particles was ∼1−3 μm. Twenty-five wt % Y-211 and 0.5 wt % CeO_2 were added to the Y-123 powder and mixed together thoroughly using a mechanical mixer for 3 h. CeO_2 was added to the precursor to refine the grain size of Y-211 inclusions in the fully processed single grain and therefore to enhance flux pinning. The mixed precursor powders were pressed uniaxially into discs both for the main green pellet and the buffer pellet, as shown in Figure 2. Details of the quantities of powder used and the dimensions of the as-pressed green pellets are given in Table 1.

As-pressed YBCO discs capped with different buffer pellets, consisting of powders of Y-123 + Y-211 + CeO_2, Y-211, and Y-211 + $Ba_3Cu_5O_8$, supported by bars of yttria-stabilized zirconia, were

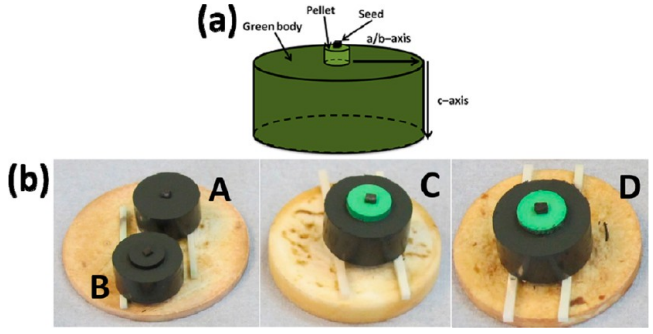

Figure 2. (a) Schematic assembly of the precursor pellet, buffer layer, and seed crystal prior to melt processing. (b) Actual arrangement of different buffer pellets on the YBCO precursor pellets for fabricating samples A−D by top-seeded melt growth (TSMG). Nd-123 seed crystals were used as seeds in each case.

DOI: 10.1021/cg501813y
Cryst. Growth Des. 2015, 15, 1472−1480

Table 1. Dimensions and Weights of Samples A–D before and after TSMG

sample code	composition of the buffer pellet	before processing			after processing	
		dia (mm)	weight of the YBCO disc (g)	weight of the buffer (g)	dia (mm)	weight of the sample (g)
A	no buffer	32	35.05	0	25.62	33.09
B	75 wt % Y-123 + 25 wt % Y-211 + 0.5 wt % CeO_2	32	35.07	0.54	25.5	33.67
C	Y-211	32	35.03	0.52	25.2	32.82
D	Y-211, $Ba_3Cu_5O_8$	32	35.04	0.52	25.45	32.79

arranged on alumina plates, as shown in Figure 2. A reference sample without a buffer pellet was also processed for purposes of comparison. Slab-shaped Nd-123 seeds, cleaved along the (00l) plane, were placed on the top surfaces of the precursor/buffer pellet assemblies, and the entire arrangements were melt-processed in a box furnace as described elsewhere.[13] Briefly, this involved heating the samples to 1054 °C and holding for 1 h to enable complete incongruent melting of the Y-123 phase into solid Y-211 and a liquid phase. The samples were then cooled rapidly to 1010 °C and then slow cooled at 0.8–0.2 °C/h to 980 °C to ensure heterogeneous nucleation and growth of the Y-123 phase. Finally, the samples were furnace-cooled to room temperature. The fully melt-processed samples were annealed in flowing oxygen at 440 °C for 150 h.

Sections of the fully processed grains were prepared for microstructural studies using a diamond saw (Minitom, Struers) and a mechanical polisher (Knuth Rotor 2 and Struers DAP-7). The microstructures of these samples were examined using an optical microscope equipped with a polarizer (Eclipse ME 600, Nikon, and Capture 2.0, DinoLite) and a scanning electron microscope equipped with EDX (S-3400, Hitachi). The top surfaces of all the samples prepared as part of this study were polished using a SiC paper based autopolisher to obtain the flat, smooth surfaces required for trapped field measurements. Each of the samples was subjected to a magnetic field of 1.3 T (generated using an electromagnet, Hirst Magnetic Instruments Ltd.), with *B* applied parallel to the *c* axis of the samples, prior to field cooling to 77 K. The applied field was then removed, and the trapped magnetic flux density on the top surface of each of the samples measured using an automatic, scanning Hall probe system comprising an array of 19 Hall probes spaced uniformly over the top surface of the samples. Further details of the trapped field measurement system can be found elsewhere.[28,4] The air gap between the sample surface and the Hall probe array in each measurement was approximately 0.8–1 mm.

3. RESULTS AND DISCUSSION

3.1. Different Buffer Pellet Composition. Photographs of four YBCO samples (samples A–D) prepared under similar conditions and capped with different buffer pellets (Figure 2 and Table 1) processed using the TSMG technique are shown in Figure 3. These images can be used to assess the quality of the samples and the general success of the melt process in each case.

3.1.1. Growth Mechanism. Samples A–D were sectioned through the sample thickness and polished using an autopolisher with an abrasive medium of grit size 1 μm. SiC abrasive paper and diamond paste were used subsequently to yield a polished surface that was smooth to within 1 μm. Low-magnification optical micrographs of the cross-sections through the complete thickness of each sample are shown in Figure 4.

It can be seen that the use of a buffer pellet aids significantly the growth of the Y-123 phase but that the detail of the growth depends critically on the construction and composition of the buffer pellet used. Typical, characteristic growth of the Y-123 phase is observed in sample A, where no buffer was used, as reported frequently elsewhere.[29,30] In this process, epitaxial

Figure 3. Top and side views of TSMG processed YBCO sample A (with no buffer pellet) and samples B, C, and D (fabricated with different buffer pellets).

growth is initiated at the position of the seed and progresses characteristically both in the *a*–*b* plane and in the *c* direction of the sample. The growth process observed in samples B–D, on the other hand, differs significantly from this standard process when buffer pellets are used, as discussed further below.

The grain growth process appears to have occurred continuously for sample B, for which the buffer pellet had the same composition as that of the main YBCO pellet. In this case, the buffer pellet behaved effectively as a large, secondary seed to enable nucleation and growth of the Y-123 phase. The advantage of this method is that the seeding becomes a lot easier, which has considerable potential for the fabrication of samples with larger diameters (>25 mm). A direct consequence of the use of a buffer layer in this way is that a relatively small seed can be used to initiate the growth process. In addition, the buffer layer/seed process is tolerant of minor imperfections of the seed, such as small distortions at the seed edges that are commonly generated during the cleaving process, which do not affect significantly the growth of the Y-123 phase in the presence of a buffer layer. This is apparent in Figure 4b, where the seed used to fabricate sample B is relatively thin and is not of any specific, regular shape. It is also apparent from this figure that the use of the buffer layer effectively widens the growth region compared to that with a conventional, non-buffered TSMG process.

DOI: 10.1021/cg501813y
Cryst. Growth Des. 2015, 15, 1472–1480

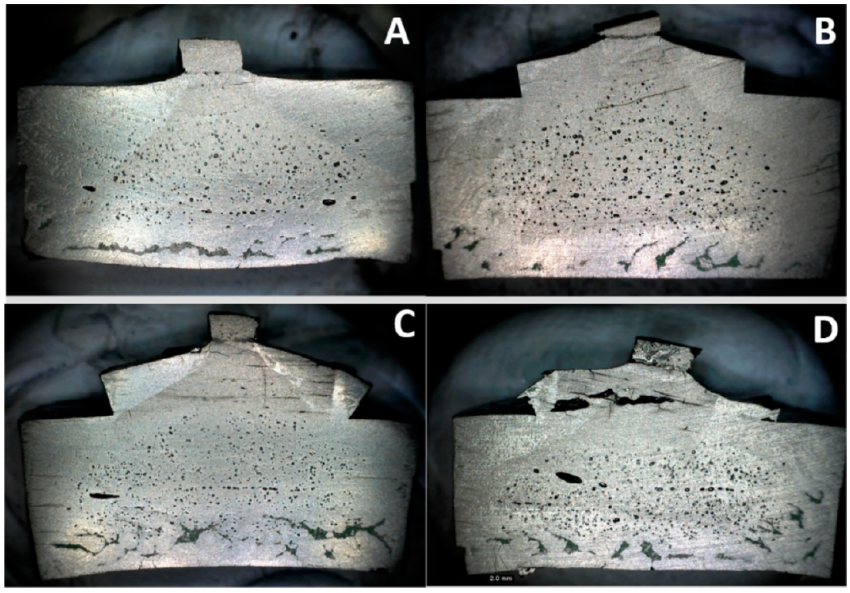

Figure 4. Optical micrographs of the cross sections of samples A–D.

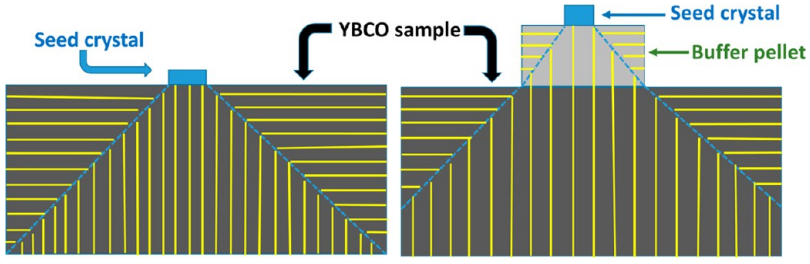

Figure 5. Schematic illustration of the growth of the Y-123 phase for samples A (with no buffer) and B (with a buffer pellet). The ability of the buffer pellet to seed a sample of larger diameter is clearly evident from this figure.

Schematic diagrams illustrating non-buffered and buffered growth for samples A and B are shown in Figure 5. It can be seen from this figure that the buffer pellet acts effectively as a single seed. This, clearly, aids the seeding process and demonstrates that a small seed is adequate to seed samples with large diameters, thus assisting the single-grain growth of YBCO.

3.1.2. Subgrain Formation in Samples C and D. The photographs of the top surfaces of samples A and B (Figure 3) show that these exhibit four facet lines that extend to the edges of the samples, which, therefore, constitute a single grain. On the other hand, subgrains are present in samples C and D, for which the buffer pellets were composed of Y-211 only and Y-211 + liquid phase, respectively. This was clearly evident when the top surfaces of these samples were polished, as can be seen in Figure 6. A possible reason for this is that the Y-211 buffer layer phase fails to melt at the processing temperature and, as a result, forms multiple nucleation centers during the growth process. The role of the buffer pellet in aiding the growth of the Y-123 phase remains evident, however, in Figure 4c,d, despite the formation of subgrains. The distortion of the buffer layer and the orientation of the seed in sample D, for which the liquid phase and the Y-211 layer in the buffer were layered separately, results from the outflow of liquid phase during the heat treatment of this sample. As a result, the seeding process itself is influenced directly and critically by the properties of the buffer layer.

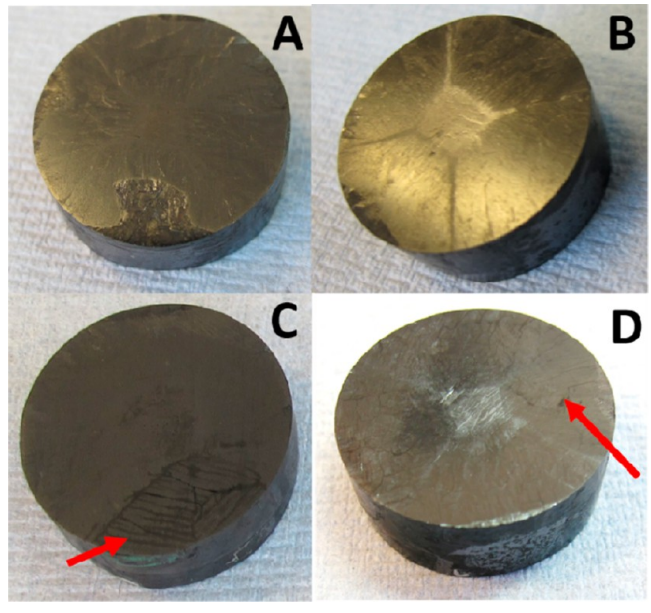

Figure 6. Polished surfaces of samples A–D (note that the buffer pellets have been removed).

3.1.3. Trapped Field Measurements. Each sample was cooled to 77 K in an applied external magnetic field of 1.3 T, and the magnitude of the trapped field on its surface was measured by a hand-held probe. Trapped field profiles were

DOI: 10.1021/cg501813y
Cryst. Growth Des. 2015, 15, 1472–1480

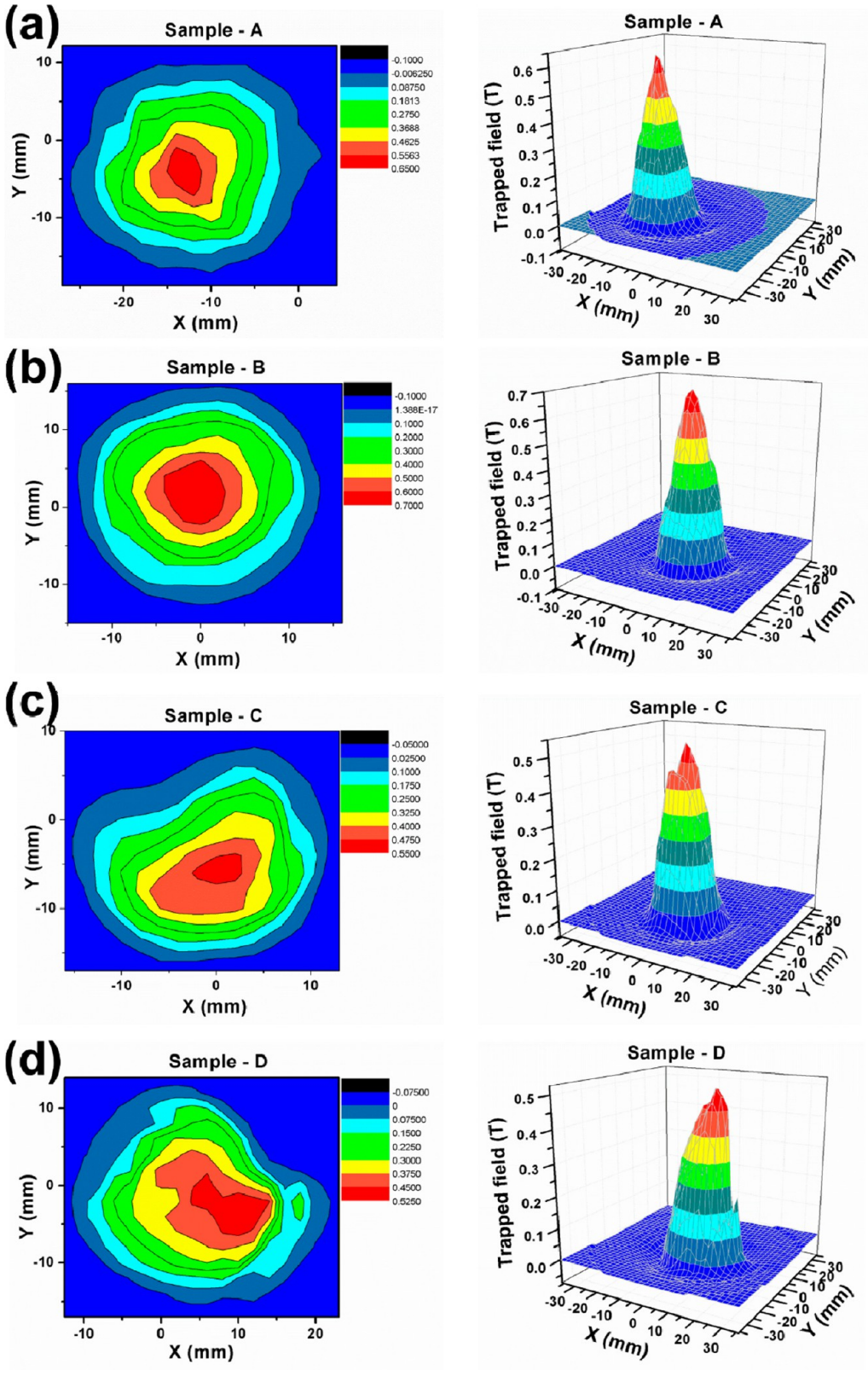

Figure 7. (a–d) Trapped field profiles at 77 K obtained for samples A–D, respectively.

recorded employing an assembly of 19 Hall probe sensors at a height of 1 mm above the sample surface, as described elsewhere.[28] The trapped field profiles (both the 3D plots and contour maps) obtained for each sample at 77 K are shown in Figure 7. It can be seen that sample B exhibits the highest trapped field of the four samples studied, with a peak field of ~0.65 T at 77 K.

In addition to exhibiting the highest peak field value, the trapped field pattern for sample B shows the highest degree of symmetry of all the samples fabricated in this study. On the

DOI: 10.1021/cg501813y
Cryst. Growth Des. 2015, 15, 1472–1480

other hand, the trapped field patterns obtained for samples C and D exhibit either multiple or distorted peaks, confirming the presence of subgrains in these samples, as discussed earlier. The maximum value of trapped field in each of the samples at 77 K is shown in Figure 8. It can be seen from the figure that the sample B exhibits the best peak performance at 77 K by some margin.

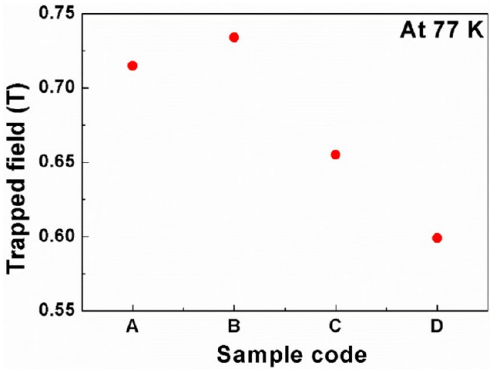

Figure 8. Trapped field measured by a hand-held Gauss meter at the surface of samples A–D.

3.1.4. Contamination Problems. It is well-known that Nd/Sm ions from Nd-123/Sm-123 seed crystals can diffuse into bulk YBCO superconductors during heat treatment to a distance of about 0.1–1 mm below the position of the seed,[24,26,31] which results in the formation of a solid solution that reduces the uniformity of $J_c(B)$ throughout the volume of the sample.[31] Nd/Sm ions substitute typically on the Ba site in the Y-123 phase, which suppresses T_c of the YBCO bulk sample, at least locally. In the present work, the best performing buffer pellet composition (sample B) has the potential to prevent, or at least inhibit, the diffusion of Nd/Sm from the seed crystal. For this purpose, the concentration of Nd in the as-grown sample was investigated by carrying out EDX studies on selected regions of samples A and B. This involved scanning the Nd concentration over several, equispaced frames of size 50 × 50 μm^2, from the surface of the sample to the bottom of its cross-section, as shown in Figure 9.

It can be seen from Figure 9 that Nd is present up to a depth of ∼1 mm from the seed/YBCO interface in sample A, corresponding to the zone within which solid solution formation occurs. The Nd concentration decreases rapidly

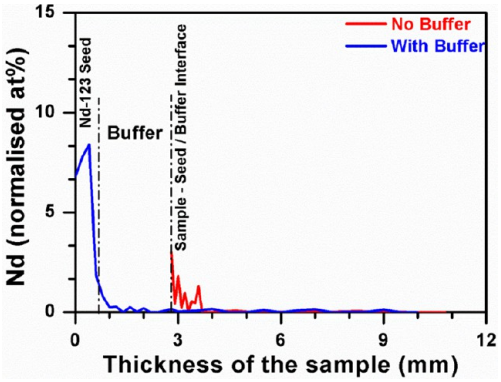

Figure 9. Nd concentration measured along the thickness of samples A (with no buffer) and B (with buffer).

with distance in sample B and disappears completely at the bottom surface of the buffer layer to yield a bulk YBCO sample free from solid solution (i.e., with only Nd present as a trace element and below the sensitivity level of the measurement).

Kim et al. established that the diffusion of Nd from the seed crystal into the bulk Y-123 matrix can be prevented by employing Y-211 buffer pellets of thickness > 3 mm,[26,31] although these authors did not investigate whether the use of the buffer resulted in the formation of subgrains in the YBCO sample. It has been established in the present study that the diffusion of Nd/Sm into the YBCO bulk is prevented by the buffer pellet configuration used for the fabrication of sample B. In addition, this configuration yields a fully processed sample that traps a greater magnetic field and inhibits the formation of subgrains. As a result, the sample B buffer pellet configuration is preferred over that of Y-211 for the fabrication of bulk YBCO samples with improved superconducting and microstructural properties.

3.1.5. Bypassing the Interfacial Stress. It is well-known that lattice mismatch effects often cause large stresses at the interface between two materials.[11,32] The fabrication of YBCO superconductors by any seeding process characteristically generates a variety of such interfaces, which, typically, are the origin of crack formation. For example, the crystallographic misfit between Nd-123 and Sm-123 seed crystal compounds with the Y-123 phase formed during the TSMG process is unavoidable. Sample B, with buffer pellet capping, however, functioned to absorb the major cracks generated at the seed/buffer interface, which resulted in a bulk YBCO sample that was almost free from severe cracks. Optical and scanning electron micrographs obtained at the seed/buffer and buffer/YBCO interfaces of sample B are shown in Figure 10. It can be seen that very few cracks are present at the buffer/YBCO interface region (Figure 10b).

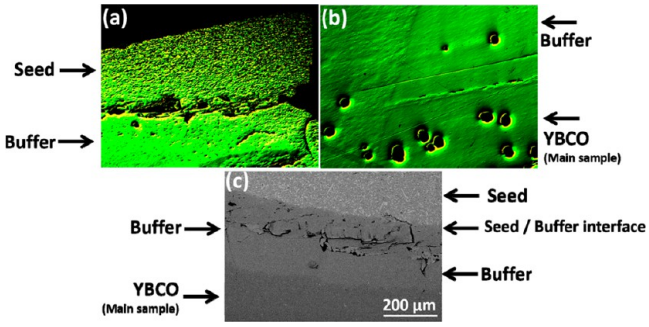

Figure 10. Optical micrographs obtained for sample B at the (a) seed/buffer and (b) buffer/YBCO interfaces. (c) Electron micrograph taken at the seed/buffer interface.

In this case, the buffer pellet together with the seed crystal acts as a single, large homoseed crystal and effectively aids the growth of the RE-123 phase. As a result, this configuration enables the buffer pellet to effectively absorb defects that occur during the initial stage of growth via lattice mismatch effects, thus inhibiting their formation in the main bulk microstructure. Typically, this optimized buffer pellet configuration can be considered to be a hybridized seeding technique that bridges both the hot seeding and cold seeding techniques while retaining the advantages of both (i.e., the ease of placing the seed crystal on the green body at room temperature and

DOI: 10.1021/cg501813y
Cryst. Growth Des. 2015, 15, 1472–1480

seeding grain growth via a crystal of the same composition as that of the parent bulk).

It is clear from these investigations that the buffer configuration adopted for sample B is the most successful for fabricating large, single grain YBCO samples by the TSMG technique. Further engineering of the aspect ratio of the buffer pellet was performed subsequently, as described below.

3.2. Geometry of the Buffer Pellet. Small pellets with different aspect ratios ($R_{h/r}$) were prepared and characterized in order to investigate the influence of geometric configuration on the effectiveness of the buffer pellets for seeding. These pellets were fabricated from YBCO precursor powders (using the same configuration for the fabrication of sample B, as mentioned above) by uniaxially pressing the constituent powders into cylindrical shapes with different geometric parameters, as summarized in Table 2. Sm-based seeds were chosen for this study in an attempt to verify the compatibility of buffer pellets compared to other available seeds. SmBCO single-crystal seeds fabricated as described elsewhere[33] were cleaved along the $a-b$ plane, sectioned into small slabs, and placed on the top surface of each of the buffer pellets, as shown schematically in Figure 2a. Essentially, the assembly of the SmBCO single-crystal seed and the buffer pellet acts as a coherent seed arrangement in the TSMG processing of bulk YBCO superconductors. Five samples, #1, #2, #3, #4, and #5, were fabricated by varying the aspect ratio of the buffer pellet from 3.0 to 1.1, as described in Table 2, corresponding to ratios of 3.0, 2.3, 1.9, 1.6, and 1.1, respectively. Photographs of the top and side surfaces of the as-processed TSMG YBCO for samples #1 to #5 grown with buffer pellets of different $R_{h/r}$ are shown in Figures 11 and 12.

Table 2. Geometric Parameters of the Buffer Pellets

	before TSMG	after TSMG		
sample no.	weight (g)	radius (mm)	height (mm)	$R_{h/r}$
#1	0.36	2.0	5.9	3.0
#2	0.30	2.2	5.1	2.3
#3	0.24	1.9	3.7	1.9
#4	0.22	1.9	3.1	1.6
#5	0.13	1.9	2.1	1.1

The geometric parameters corresponding to each of the samples are given in Table 2. It is evident from Figures 11 and 12 that the growth of the Y-123 phase is more complete for a buffer pellet aspect ratio of 1.1 (sample #5) and that incomplete growth, to varying degrees, is observed for the other samples. Subgrains form randomly in the case of sample #1, which has the highest $R_{h/r}$ of 3.0 for the buffer pellet, and irregular facet lines are present in the top surface of the sample. The orientation of the buffer pellet, and hence the driver of the seeding process, appears to improve and aid better the growth of the Y-123 phase as the aspect ratio decreases from 3.0 to 1.1. This is perhaps due to the fact that the effect of seeding through the buffer layer is active when $r = h$ for the buffer pellet. This ensures that there is no problem associated with undercooling, as occurred for sample #1, while, at the same time, the crack/diffusion problems of associated with Nd/Sm diffusing from the seed crystal to the parent bulk are eliminated to a large extent. Sample #5, on the other hand, exhibits well-defined, 4-fold faceted growth symmetry of the Y-123 phase.

It can be seen further from Figure 12 that the extent to which the processed buffer pellets tilt reduces progressively from samples #1 to #5, thereby enabling more controlled, stable growth of the Y-123 phase. The titled growth morphology of the buffer pellet might be the source of the double-faceted lines in samples #2, #3, and #4. It is well-known that any small misorientation during seeding can affect critically the grain growth of the Y-123 phase.[34] It can be concluded, therefore, that the growth configuration of sample #5, where $r \approx h$ or $R_{h/r} \approx 1$, is close to optimum for the growth of a single YBCO grain of good quality.

The serious failure of sample #1 (with $R_{h/r}$ of 3.0) is understandable given the height of the buffer pellet (5.9 mm) after heat treatment. Such a large buffer pellet height results in a relatively longer time for an efficient seeding process to occur since the growth rate of the Y-123 phase is very small, of the order of 0.2−0.5 mm/h.[35] In this case, therefore, the seeding process is dominated by undercooling effects in this sample, which result in the formation of a large number of subgrains.

Figure 11. Top view of the TSMG processed YBCO samples #1, #2, #3, #4, and #5 with buffer pellets of different aspect ratios (3.0 to 1.1).

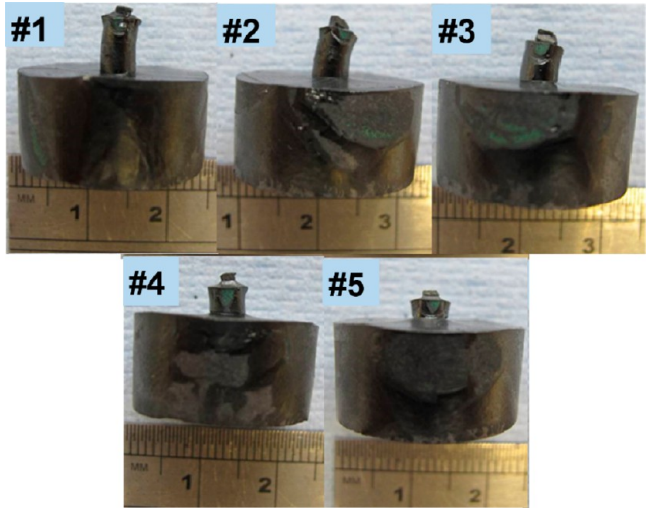

Figure 12. Side view of YBCO samples (#1 to #5) fabricated with buffer pellets of different $R_{h/r}$.

DOI: 10.1021/cg501813y
Cryst. Growth Des. 2015, 15, 1472−1480

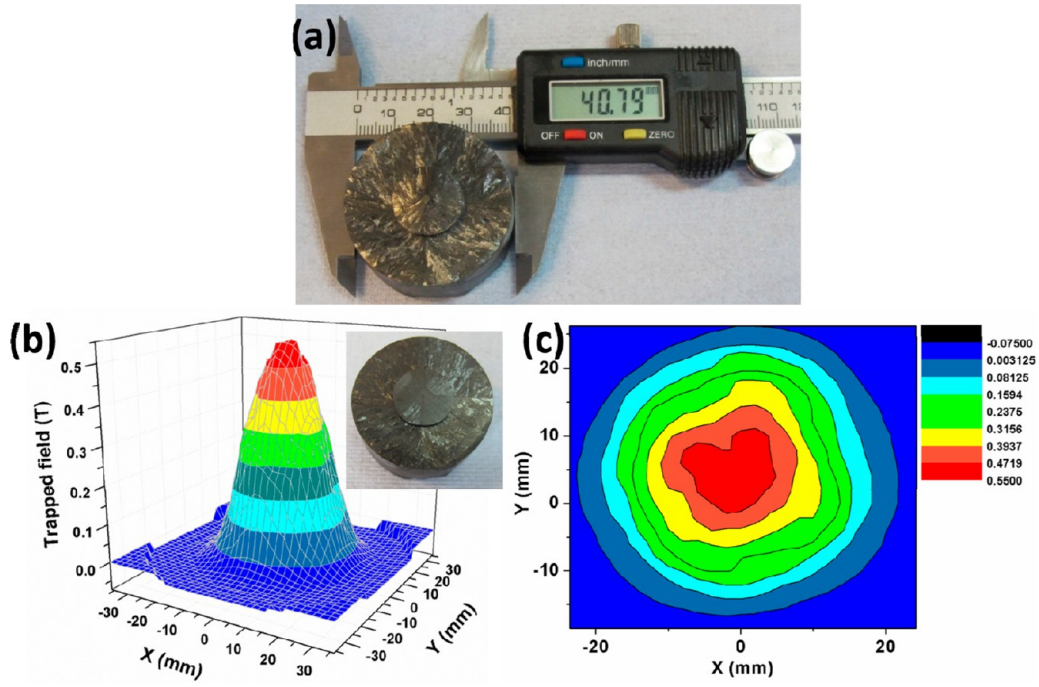

Figure 13. (a) Photograph of a large, single-grain YBCO sample of 40.8 mm diameter. Trapped field profiles: 3D lobe (b) and 2D contour map (c) for the sample at 77 K. The polished sample surface on which the trapped field profile was measured is shown in the inset of (b).

Figure 14. Photographs of a batch of YBCO samples fabricated using capped buffer pellets. Single-grain growth of the Y-123 phase is indicated by the presence of the four facet lines in each sample.

3.3. Fabrication of Large-Sized Bulk YBCO Superconductors. Attempts have been made by several researchers to fabricate large single grains of (RE)BCO in general, and YBCO in particular, but with very limited success when the diameter of the sample exceeds around 25 mm. Subgrains form very easily in samples of this size, which results, typically, in the production of multigrained bulk superconductors with an involved and optimized processing methodology.

A large-sized YBCO bulk superconductor of ~40.8 mm diameter was fabricated in the present study by TSMG using an optimized buffer pellet configuration of identical composition to that of the YBCO sample (75 wt % Y-123 + 25 wt % Y-211 + 0.5 wt % CeO_2), as shown in Figure 13a. The trapped field profile measured at a height of 2.2 mm above its top surface shown in Figure 13b confirms the single-grain nature of this sample. This is relatively low compared to that shown in Figure 8 due to the larger distance between the surface of the sample and the Hall probe.

3.4. Batch Processing of Samples with Buffer Pellets. More than 25 YBCO samples of diameter varying between 25 and 35 mm were fabricated using the methodology developed in this investigation with a success rate of 95% in order to verify the reproducibility of the process. This involved capping the pressed discs with buffer pellets composed of Y-123, Y-211, and CeO_2 powders and using Nd-123 seeds. The buffer pellet/Nd-123 seed combination acts effectively as a single seed and aids the growth of the Y-123 phase. The introduction of the buffer layer seeding technique has increased the success rate of the melt processing of larger diameter samples in this study to 95%. Photographs obtained from the YBCO samples fabricated following this methodology are shown in Figure 14 for purposes of illustration.

4. SUMMARY AND CONCLUSIONS

An optimized, effective seeding process is essential for controlled and reproducible growth of single-grain YBCO

DOI: 10.1021/cg501813y
Cryst. Growth Des. 2015, 15, 1472−1480

throughout the entire sample using the top-seeded melt growth technique. A methodology has been developed to increase the success rate significantly of melt processing single-grain YBCO bulk superconductors using the TSMG process. This involved investigating systematically different buffer pellet arrangements to serve as effective nucleation and growth sites for the Y-123 phase in bulk YBCO. The geometric aspect of the buffer pellet was also varied, and the best configuration was identified from the resulting YBCO grain growth morphologies, with the buffer pellet aspect ratio $R_{h/r}$ of ∼1 yielding the best seeding performance. In particular, this configuration did not suffer from the effects of tilting during single-grain growth and, simultaneously, avoided serious microstructural defects associated with crystallographic misorientation of the seed. A large, YBCO sample of 40.8 mm diameter was fabricated successfully using the optimized buffer pellet configuration. In addition, a number of YBCO samples with diameters in the range 25−35 mm were grown successfully using this optimized buffer seeding technique. This enabled subsequently the fabrication of large, single-grain bulk YBCO superconductors with a success rate in excess of 95%. It is reasonable to speculate that, by employing a buffer pellet, larger single grains can be grown by adjusting the seed/buffer pellet dimensions and the thermal window for melt growth. The buffer pellet and seed crystal arrangement effectively forms a single seed, which overcomes the problem of serious lattice mismatch that is otherwise present. The present work has significant potential for application to the practical fabrication of large, single-grain YBCO components for a range of engineering and technological applications.

AUTHOR INFORMATION

Corresponding Author

*E-mail: dkn23@cam.ac.uk.

Notes

The authors declare no competing financial interest.

ACKNOWLEDGMENTS

The authors are grateful to the King Abdulaziz City of Science and Technology (KACST), Saudi Arabia, and to the Engineering and Physical Sciences research Council (EPSRC) for financial support of this research.

REFERENCES

(1) Cardwell, D. A. *Mater. Sci. Eng., B* **1998**, *53*, 1−10.
(2) Diko, P. *Supercond. Sci. Technol.* **2000**, *13*, 1202−1213.
(3) Ikuta, H.; Mase, A.; Yanagi, Y.; Yoshikawa, M.; Itoh, Y.; Oka, T.; Mizutani, U. *Supercond. Sci. Technol.* **1998**, *11*, 1345−1348.
(4) Durrell, J. H.; Dennis, A. R.; Jaroszynski, J.; Ainslie, M. D.; Palmer, K. G. B.; Shi, Y.-H.; Campbell, A. M.; Hull, J.; Strasik, M.; Hellstrom, E. E.; Cardwell, D. A. *Supercond. Sci. Technol.* **2014**, *27*, 082001.
(5) Nariki, S.; Sakai, N.; Murakami, M.; Hirabayashi, I. *Supercond. Sci. Technol.* **2004**, *17*, S30−S35.
(6) Cardwell, D. A.; Hari Babu, N. *Phys. C* **2006**, *445*, 1−7.
(7) Salama, K.; Lee, D. F. *Supercond. Sci. Technol.* **1994**, *7*, 177−193.
(8) Meslin, S.; Iida, K.; Hari Babu, N.; Cardwell, D. A.; Noudem, J. *Supercond. Sci. Technol.* **2006**, *19*, 711−718.
(9) Devendra Kumar, N.; Rajasekharan, T.; Gundakaram, R. C.; Seshubai, V. *IEEE Trans. Appl. Supercond.* **2011**, *21*, 3612−3620.
(10) Mei, L.; Boyko, V. S.; Chan, S.-W. *Phys. C* **2006**, *439*, 78−84.
(11) Shi, Y. H.; Hari Babu, N.; Iida, K.; Yeoh, W. K.; Dennis, A. R.; Cardwell, D. A. *Supercond. Sci. Technol.* **2009**, *22*, 075025.
(12) Nariki, S.; Sakai, N.; Murakami, M. *Phys. C* **2003**, *392−396*, 516−520.
(13) Hari Babu, N.; Jackson, K. P.; Dennis, A. R.; Shi, Y. H.; Mancini, C.; Durrell, J. H.; Cardwell, D. A. *Supercond. Sci. Technol.* **2012**, *25*, 075012.
(14) Izumi, T.; Nakamura, Y.; Shiohara, Y. *Adv. Supercond.* **1991**, *5*, 429−432.
(15) Salama, K.; Selvamanickam, V. *Supercond. Sci. Technol.* **1992**, *5*, S85−S88.
(16) Nakamura, Y.; Ooishi, Y.; Kato, K.; Inada, R.; Oota, A. *IEEE Trans. Appl. Supercond.* **2007**, *17*, 2988−2991.
(17) Shi, Y. H.; Hari Babu, N.; Cardwell, D. A. *Supercond. Sci. Technol.* **2005**, *18*, L13−L16.
(18) Tang, C.; Yao, X.; Ju, J.; Rao, Q.; Li, Y.; Tao, B. *Supercond. Sci. Technol.* **2005**, *18*, L31−L34.
(19) Cheng, L.; Li, T.; Yan, S.; Sun, L.; Yao, X.; Puzniak, R. *J. Am. Ceram. Soc.* **2011**, *94*, 3139−3143.
(20) Zhou, D.; Xu, K.; Hara, S.; Li, B.; Deng, Z.; Tsuzuki, K.; Murakami, M. *Supercond. Sci. Technol.* **2012**, *25*, 025022.
(21) Peng, B.; Cheng, L.; Zhuang, Y.; Xu, H.; Yao, X. *Phys. C* **2014**, *496*, 11−13.
(22) Xu, H. H.; Chen, Y. Y.; Cheng, L.; Yan, S. B.; Yu, D. J.; Yao, X. *Supercond. Sci. Technol.* **2012**, *25*, 035014.
(23) Kim, C. J.; Jee, Y. A.; Hong, G. W.; Sung, T. H.; Han, Y. H.; Han, S. C.; Kim, S. J.; Bieger, W.; Fuchs, G. *Phys. C* **2000**, *331*, 274−284.
(24) Jee, Y. A.; Hong, G. W.; Kim, C. J.; Sung, T. H. *Supercond. Sci. Technol.* **1998**, *11*, 650−658.
(25) Chen, S. Y.; Hsiao, Y. S.; Chen, C. L.; Yan, D. C.; Chen, I. G.; Wu, M. K. *Mater. Sci. Eng., B* **2008**, *151*, 31−35.
(26) Li, T.; Cheng, L.; Yan, S. B.; Sun, L. J.; Yao, X.; Yoshida, Y.; Ikuta, H. *Supercond. Sci. Technol.* **2010**, *23*, 125002.
(27) Shi, Y. H.; Dennis, A. R.; Cardwell, D. A. *Supercond. Sci. Technol.*, in press.
(28) Withnell, T. D.; Hari Babu, N.; Ganney, I.; Dennis, A. R.; Cardwell, D. A. *Mater. Sci. Eng., B* **2008**, *151*, 79−83.
(29) Koblischka Veneva, A.; Holzapfel, C.; Mücklich, F.; Koblischka, M. R.; Hari Babu, N.; Cardwell, D. A. *J. Phys.* **2006**, *43*, 527−530.
(30) Reddy, E. S.; Hari Babu, H.; Shi, Y.-H.; Cardwell, D. A. *J. Eur. Ceram. Soc.* **2005**, *25*, 2935−2938.
(31) Kim, C. J.; Lee, J. H.; Park, S. D.; Jun, B. H.; Han, S. C.; Han, Y. H. *Supercond. Sci. Technol.* **2011**, *24*, 015008.
(32) Pathak, S. K.; Yeoh, W. K.; Hari Babu, N.; Shi, Y.-H.; Iida, K.; Strasik, M.; Cardwell, D. A. *Phys. C* **2009**, *469*, 1173−1177.
(33) Shi, Y.-H.; Hari Babu, N.; Iida, K.; Cardwell, D. A. *J. Phys.* **2008**, *97*, 012250.
(34) Zhai, W.; Shi, Y.-H.; Durrell, J. H.; Dennis, A. R.; Rutter, N. A.; Troughton, S. C.; Speller, S. C.; Cardwell, D. A. *Supercond. Sci. Technol.* **2013**, *26*, 125021.
(35) Shi, Y.-H.; Yeoh, W. K.; Dennis, A. R.; Hari Babu, N.; Pathak, S. K.; Xu, Z.; Cardwell, D. A. *J. Phys.* **2010**, *234*, 012039.

DOI: 10.1021/cg501813y
Cryst. Growth Des. 2015, 15, 1472−1480